GeoAmericas2020
4th PAN AMERICAN CONFERENCE ON GEOSYNTHETICS
26-29 APRIL 2020 • RIO DE JANEIRO • BRAZIL

Evaluation of factors affecting geomembrane strain caused by tire derived aggregate and gravel in landfill barrier applications

B.A. Marcotte, Department of Civil, Geological, and Environmental Engineering, University of Saskatchewan, Saskatoon, Canada
I.R. Fleming, Department of Civil, Geological, and Environmental Engineering, University of Saskatchewan, Saskatoon, Canada

ABSTRACT

Geomembranes are used in waste containment barrier systems to limit to movement of contaminants. The geomembrane is placed over a clay liner, and a drainage blanket consisting of highly permeable coarse aggregate is placed above the geomembrane for removal of leachate to control the hydraulic head. Coarse uniform gravel is typically used as a drainage layer. Where such gravel is scarce or expensive, there has been a trend in recent years to use tire derived aggregate (TDA). Differential loading of the geomembrane by the large TDA or gravel particles over a yielding compacted-clay subgrade leads to indentations. The high localised strain that occurs around indentations may lead to stress cracking. Protection layers are now designed to minimize the development of high localised strain rather than ductile punctures.

A photogrammetry method was developed and performed on over 60 laboratory tests to evaluate variables controlling geomembrane strain. Clay properties play a key role in the magnitude of resulting strains. Fast loading rates (over less than 1 hour) resulted in higher strains when compared to slow incremental loading (over 6 months). The role of the clay in the deformation of geomembranes is a significant factor that must be taken into account when designing composite barrier systems. The final component of this study involved a comparison of tensile strain induced by TDA and gravel. High-localised strain from TDA was less than for angular gravel, and substantially less bending strains occurred, indicating that differences in indentation size and shape from different aggregates should be considered.

1. INTRODUCTION

Geomembranes are used to limit contaminant transport out of waste containment facilities and landfills worldwide. The geomembrane acts in unison with a clay liner (either compacted or a geosynthetic) to form a composite liner (Rowe 2005). An aggregate drainage layer placed above allow for removal of leachate and reduction in hydraulic head. Large uniform aggregate is preferred as the decreased surface area reduces the potential for bacterial induced clogging (Fleming et al. 1999). Sourcing large gravel required for landfill drainage layers can be challenging depending on the geologic history near the facility.

Tire derived aggregate (TDA) is manufactured by shredding or cutting the tires into large pieces. TDA is an appealing alternative as it is both cost effective and provides a method of recycling tires (which are often prohibited from being landfilled otherwise). TDA undergoes significant vertical compression under load, but still has sufficient permeability and porosity to function as a drainage layer (Adesokan et al. 2019). However, many of the TDA pieces contain protruding wires that are a risk of puncturing the geomembrane. Recent work has demonstrated that heavy nonwoven geotextile (greater than 1088 g/m^2) or soil protection layers combined with rigorous TDA quality control are required to minimize the number of expected 1 mm diameter punctures to fewer than 15 per hectare (Marcotte & Fleming 2018a,b, 2020). This number of punctures may or may not be acceptable for every facility.

Even if a few ductile (large-strain) punctures occur from construction damage or wires in the TDA, gravel, or construction damage (Nosko & Touze-Foltz 2000), the composite system can still perform adequately to reduce contaminant movement (Rowe 2012). However, the ultimate failure of the geomembrane is likely to occur due to stress cracking (Rowe et al. 2019). Geomembranes may develop many brittle ruptures, referred to as stress cracks, if sustained small tensile strains occur in (Abdelaal et al. 2014; Hsuan & Koerner 1998; Peggs et al. 2005). Strains in the geomembrane are critical for long-term performance as areas of exceedingly high strain my represent thousands of hole per hectare (Abdelaal et al. 2014), far exceeding the expected holes from installation damage.

The time to stress cracking depends not only on the magnitude of the strains, but on the geomembrane, temperature, and leachate conditions (Abdelaal et al. 2014; Ewais et al. 2014). The magnitude of the geomembrane strains is a function of

the geomembrane thickness (Tognon et al. 2000), the aggregate size and shape (Brachman & Gudina 2008), the protection layer above (Brachman & Sabir 2013; Narejo et al. 1996; Tognon et al. 2000) and the clay properties below (Marcotte & Fleming 2019). The maximum allowable tensile strain depends both on the design lifespan and the expected conditions. Rowe et al. (2019) suggested a target maximum allowable strain of 3% (considering bending strains) for the base of a nuclear waste facility designed for 550 years (although the site temperature of 10° would be far less than an active landfill). At this time, 4% is a relatively accepted threshold for geomembrane strains (Rowe and Yu 2019). It is important to consider all variables in the development of geomembrane strains, but this is often challenging due to the large number of variable combinations.

The objective of this paper is to highlight some new insights into the distribution of localised high strain induced in a geomembrane by irregular point loading from aggregate (both gravel and TDA). Specifically, the properties of the clay underliner, particularly the strength and stiffness, play a key role in the development of localised strain in the geomembrane. The mechanical properties of the clay reflect not only the degree of compaction and the resulting dry density, but also the mineralogy and index propertied of the clayey soil. A second key consideration is the loading rate – the response of the clay-geomembrane system to slow drained loading is considerably different than observed when load is applied more rapidly as has been the case for most of the published laboratory testing (Tognon et al. 2000; Rowe et al. 2013; Brachman & Gudina 2008; Marcotte & Fleming 2019). Other important considerations that will be addressed in this paper include the thickness of the geomembrane and performance of different protection layers in limiting strains for different gravels and TDA.

2. METHODOLOGY

2.1 Laboratory Device

A variation of the pressure test (Brummerman et al. 1994) is most commonly performed to evaluate geomembrane strains. In the pressure test, a geomembrane is placed above a deformable subgrade and the desired aggregate is placed on the geomembrane/protection layer combination. Load is increased to simulate the high pressures present at the base of landfills. Custom pressure cylinders, one 900 mm and two 400 mm in diameter, were constructed as shown in Figure 1. The large average (96 mm) size of TDA, as shown in Figure 1 dictated the size of the 900 mm apparatus.

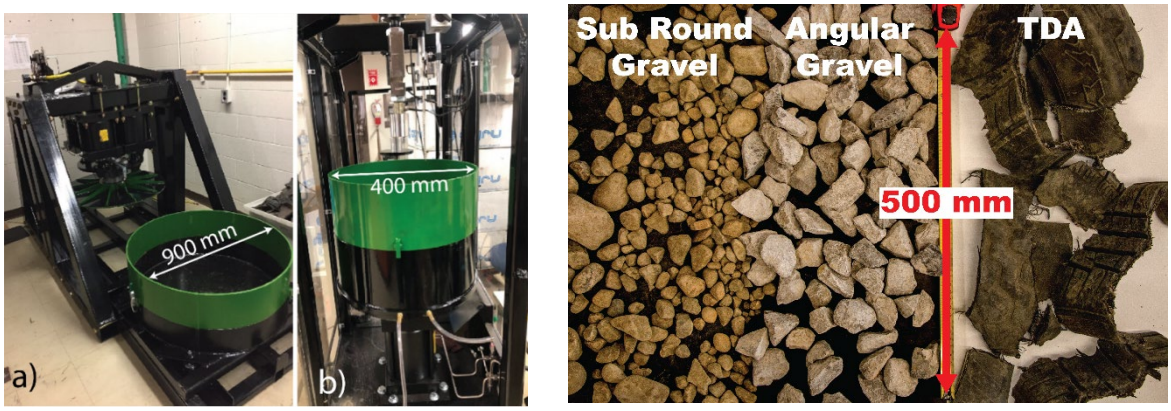

Figure 1: Test devices and aggregate used in geomembrane strain research a) large diameter device primarily for TDA; b) small diameter device for gravel c) aggregates

Each cylinder had a removable upper ring (green) above a 150 mm deep lower ring to facilitate compacting and smoothing of clay. Pneumatic actuators applied the force. Connection to a small computer (Raspberry Pi) allowed for simple automation and control of applied pressure and loading rates (see Yesnik et al. 2019). In the smaller (400 mm) cells, the bottom was machined to allow for the consolidation of clay to occur.

2.2 Clay soil subgrades

Compacted clay was used in landfill facilities prior to the widespread use of geomembranes. The research dictated that the clay be compacted at a higher water content than Standard Proctor optimum moisture to ensure that the hydraulic conductivity is sufficiently low (Benson and Daniel, 1990; Benson et al., 1999). However, having a clay with a higher compacted water content will reduce both the undrained shear strength and stiffness (due to a reduction in matric suction and density).

Until recently, limited research had been conducted on geomembrane strains above clays with different properties. A large body of research was conducted on a low-plasticity till (Halton Till) from south-central Ontario in eastern Canada (Brachman & Gudina, 2008; Brachman & Sabir, 2013; Rowe et al. 2013; Tognon et al. 2000). The consistency of the soil used between each of these studies was advantageous in comparing variables in the large list of possible combinations (contact pressure, applied pressure, protection layers, aggregates etc); however, the results only applied to a specific soil.

To evaluate the role of the clay Marcotte & Fleming (2019) obtained samples of clayey soils from several different widely dispersed regions of Canada. Each of the clays was dried, crushed, and then mixed with distilled water to a prescribed target moisture content. The clays were placed in a humidity-controlled environment for at least 48 hrs to relatively equal distribution of water. Each soil was weighed prior to placement and soil samples were taken and dried to calculate water content and determine densities. The clay was then compacted and a steel rolling pin was used to smooth the surface.

Evaluation of geomembrane strain directly is difficult as the geomembrane rebounds upon removal of any load applied. Many researchers use a lead sheet placed below the geomembrane to capture the profile of the geomembrane under load (ex. Brachman et al. 2018; Tognon et al. 2000.; Seeger & Muller 1996). More recently, a photogrammetric method has been used to directly capture the deformed clay surface as a surrogate for the geomembrane deformations (Adesokan et al. 2018; Marcotte & Fleming 2017, 2018a,b) which involves directly “scanning” the clay surface deformations, foregoing the need for the lead sheet. However, the photogrammetric method requires the clay be as smooth as possible as any imperfections can lead to misinterpreted high strains. A thin polyethylene wrap is placed between the smooth geomembrane and the clay to prevent clay from adhering to the geomembrane

2.3 Photogrammetry

Photogrammetry is the science of making measurements from photographs. When multiple photographs are taken of the same object from different angles, the data contained within the photographs can be used to triangulate the location of points and determine locations of the cameras. The accuracy of photogrammetry is a function of the equipment used, distance to the object, and number and quality of overlapping photos.

When pressure was applied to the aggregate above the geomembrane/protection layer, the clay surface was deformed representing the geomembrane under load. The deformed clay was coloured with spray paint in a random fashion, as photogrammetry algorithms work best with unique pixels rather than uniform colors. Placement of a levelled scale bar near the clay provided a reference scale and coordinates to develop the digital elevation map. Approximately 35-60 photographs (depending on test size) were taken and processed using commercial software (Agisoft 2019). Images of the camera locations, point cloud, and resulting mesh are shown in Figure 2 for a 900 mm test with TDA.

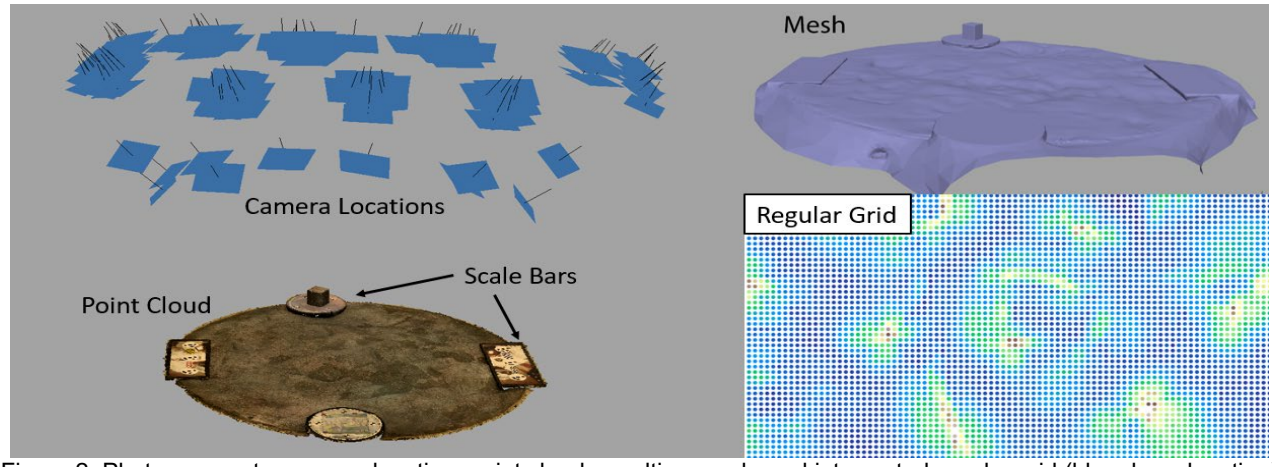

Figure 2: Photogrammetry camera location, point cloud, resulting mesh, and interpreted regular grid (blue=low elevation)

The photogrammetry procedure results in a dense point cloud with over 100 points per square millimeter (Marcotte & Fleming 2019). Using the open source coding language Python, the point cloud is reduced into a defined regularly spaced grid to facilitate the calculation of strain, as shown in Figure 2.

2.4 Approximated Geomembrane Strains Calculations

The current best practice for evaluating geomembrane strains indirectly from a profile is the method developed by Tognon et al. (2000). Tognon’s method considers the membrane and bending strain from numerical approximations. The

membrane strain assumes zero radial displacements and that the geomembrane is displaced only in the vertical direction; it can be approximated using a uniform spacing (Δx) of the vertical locations (z), the membrane strain (ε_M) can be approximated by eq. 1. The bending strain considers the different strain the fibers undergo through the thickness of the geomembrane (Brachman & Eastman, 2013). The strains will be greatest at the surfaces and zero in the middle of the geomembrane cross section and is approximated by a second-order finite difference approximation in eq. 2.

$$\varepsilon_M = \sqrt{\left[1 + \left(\frac{1}{2\Delta x}[z_{i+\Delta x} - z_{i-\Delta x}]\right)\right]} - 1 \qquad (1)$$

$$\varepsilon_B = \frac{m}{(\Delta x)^2}[z_{i+\Delta x} - 2z_i + z_{i-\Delta x}] \qquad (2)$$

Where m is the distance from the middle plane of the geomembrane. The resulting strain is the sum of the membrane and bending strain. Rather than manual selection of indentations to be measured, Hornsey & Wishaw (2012) developed a grid method, which was adapted by Marcotte & Fleming (2018) to include bending strains. Once a surface profile of the geomembrane is obtained, the elevation values are interpolated onto a uniform grid in x and y directions, as shown in Figure 2. The membrane and bending strains are then performed for each node in eight directions: four diagonal and four orthogonal for both top and bottom bending strains. The maximum calculated strain is then assigned to that node and calculations proceed across the entire surface.

2.5 Strain Area Distribution (SAD) curves

The concept of strain area distribution (SAD) curves was first proposed by Hornsey & Wishaw (2012) as a way of visualizing the distribution of geomembrane strain. Since strain is calculated on a regular grid across the entire surface, as shown by the map in Figure 3 (left), the cumulative area greater than a specified strain can be represented as a percentage of the total area. The SAD curve in Figure 3 (right) allows for quantitative comparisons between tests to be made by evaluating the area greater than a specified strain.

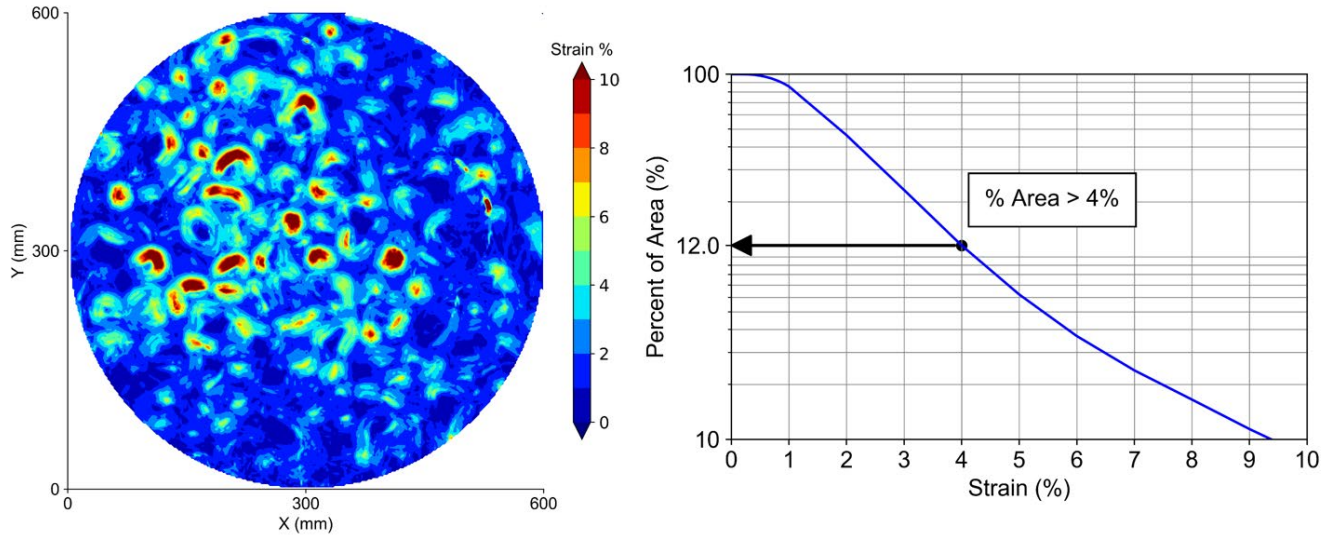

Figure 3: Strain distribution map and strain area distribution (SAD) plot with point showing the percent of the area greater than 4% strain (Test conditions: Battleford Till, 1080 g/m^2 geotextile protection, 2.0 mm geomembrane, angular gravel)

For example, if a 4% strain threshold is assumed a reasonable upper threshold for geomembrane stress cracking, approximately 12% of the area exceeds this threshold for the test conditions shown in Figure 3. The SAD distributions are a quantitative measure of geomembrane strain without subjectively selecting individual dimples to measure. For the purpose of comparing results, a 4% strain threshold will be used for the duration of paper.

3. RESULTS AND DISCUSSION

3.1 Role of the Clay

To evaluate the role of the clay in the formation of geomembrane strains, the 6 soils described by Marcotte and Fleming (2019) were compacted at different water contents relative to optimum (W-Wopt). A 1.5 mm smooth HDPE geomembrane was placed above the soils followed by a 400 g/m^2 protection layer. A 400 g/m^2 protection layer is without a doubt insufficient to prevent strains exceeding 4%, but by selecting a consistently light protection layer between tests,

the differences in the clay could be amplified. Angular gravel between 31.5 and 50.8 mm was placed above the protection layer. Further details about the test program can be found in the paper by Marcotte & Fleming (2019). Multiple tests were completed on each soil at different water contents while keeping the compactive energy constant. The resulting strains were determined to be a function of the compacted water content, as well as the index properties as shown in Figure 4.

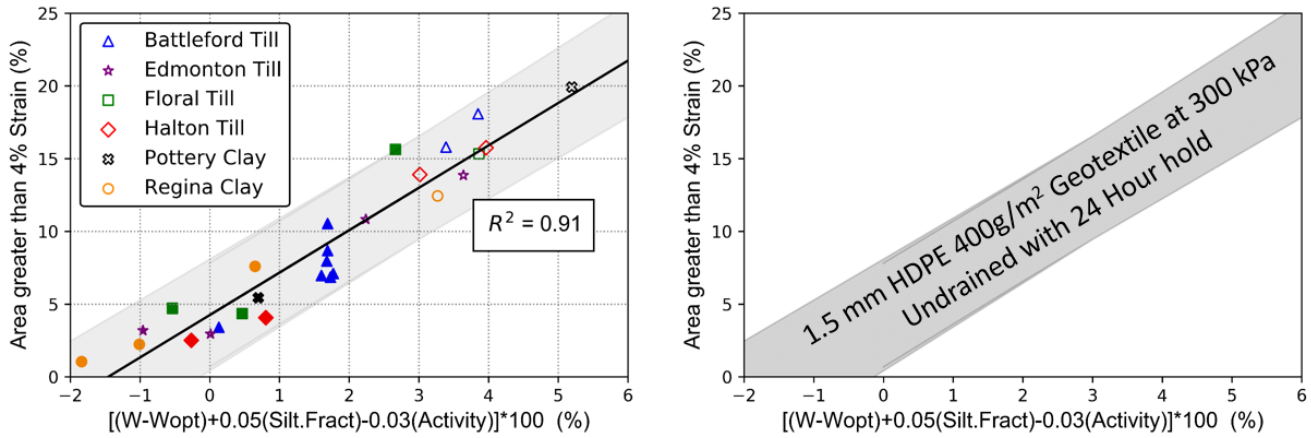

Figure 4: Role of the clay on geomembrane strains (Test constants: 300 kPa applied load; rapid loading; 24 hour hold; 400 g/m^2 protection layer; angular gravel) (modified from data by Marcotte and Fleming 2019)

The geomembrane deformed and strain differently depending on the clay conditions below. More specifically, an increase in water content led to an increase in area of geomembrane strains exceeding 4%, which is consistent with others (Rowe et al. 2013, Brachman et al. 2018). However, index soil properties such as silt fraction and activity could also be used as an indicator of strain. Clay soils with a high activity tended to fall to the right of line of best fit (indicating less strain as compared to others soils), whereas soils high in silt tended to fall to the left. The results of Figure 4 demonstrate that not only is the geomembrane, protection layer, and clay water content important, but also the type and index properties of the clay itself.

The correction factor of Figure 4 demonstrates that the strains developed in the geomembrane is relatable to the clay in a predictable pattern. Although a large number of tests were completed, this represents only a single shaded “band” of geomembrane strains in Figure 4 for a specific test pressure, loading rate, protection layer, and geomembrane thickness. The shaded band in Figure 4 will be shown in other Figures to compare other factors and the influence on the development strains relative to this specific case.

3.2 Loading Rate

The geomembrane deformation is a function of the cushioning ability of the protection layer, and the mechanical properties of both the geomembrane and clay liner below. The polymer geomembrane exhibits a viscoelastic response when subject to load. The clay liner also exhibits a time-dependent response as consolidation occurs below the stress concentrations caused by the aggregate. It has been established that consolidation should be accounted for, and sufficiently long tests are required to ensure the geomembrane and clay time-dependent responses have reached an equilibrium (Brachman & Sabir 2010; Hornsey and Wishaw 2012). Some have recommended that shorter test times are unconservative and that a factor of safety or higher test temperatures must be used to ensure the geomembrane strains fully (Sabir & Brachman 2012; Seeger & Muller 1996).

However, since the drained and undrained response of clayey soils to loading are different, the rate of loading may significantly influence the resulting geomembrane strain (ie. different stress paths during drained and undrained loading). In a municipal landfill, filling of waste may not occur rapidly, but rather slowly over months and years. This is not always the case for industrial landfills or special wastes, and loading rate effects should be considered on a case-by-case basis.

To simulate the slow loading of a landfill, a 25 kPa stepped loading function as shown in Figure 5 was applied through a Raspberry Pi connected to an electronic air regulator. The air regulator supplied the pressure to the cylinder to increase the load from in 25 kPa increments over a 12 hour span every 11 days. The spacing of 11 days was selected as the estimated time to 95% consolidation for both Battleford and Halton Till (Cv selected from the 400 kPa load step in oedometer testing). The 11 days was considered conservative to limit excess pore water pressure below the 25 kPa due to the increment steps.

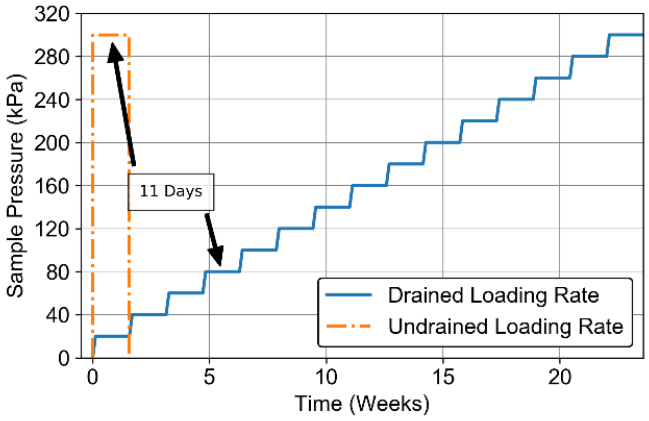

Figure 5: Loading rate for drained and undrained tests

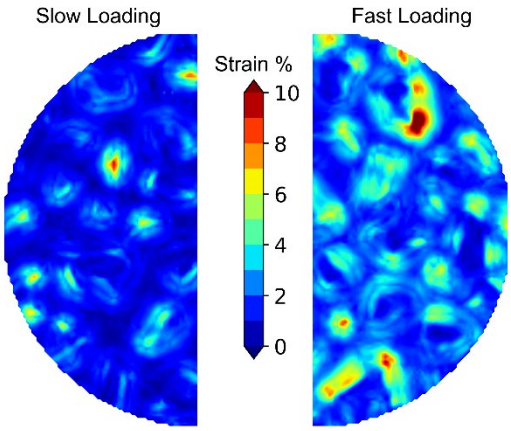

Figure 6: Strain map for slow and fast loading of Halton Till

To compare, a total of four tests were completed using Battleford and Halton till compacted to identical conditions. A relatively light 544 g/m^2 nonwoven geotextile protection was used. The undrained tests were loading as quickly as possible (<5 min) to 300 kPa and then held for a period of 11 days to allow consolidation to occur. The drained tests followed the loading rate and sequence given in Figure 5, and then held at the final load of 300 kPa for at least 11 days. The resulting strain map for Halton till is shown in Figure 6 and SAD curves and the points for both soils are shown in Figure 7.

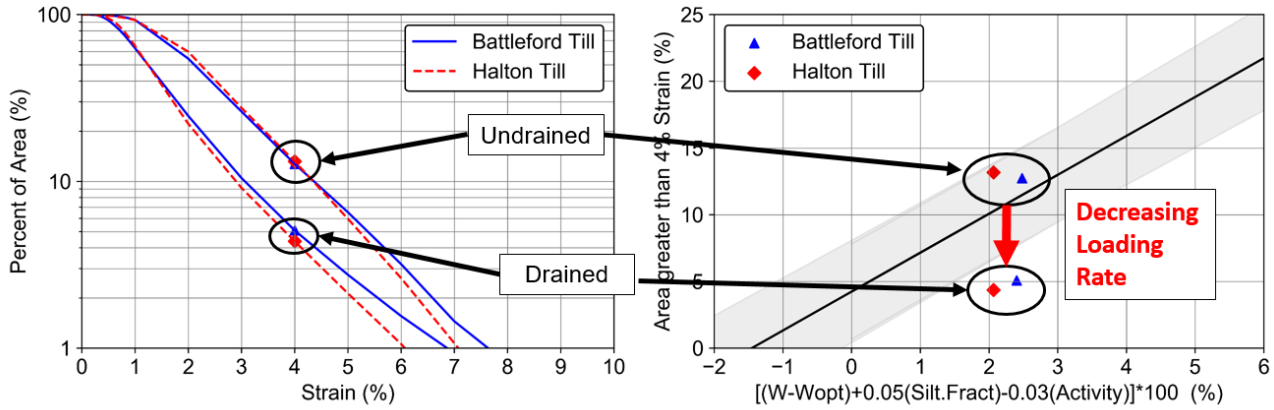

Figure 7: Effect of loading rate on geomembrane strain (Test constants: 300 kPa applied load; 544 g/m^2 protection layer; angular gravel; 1.5 mm geomembrane; soil water content and shear strength)

The undrained tests fall near the line of best fit for the 400g/m^2 geomembrane tests. One would expect the heavier protection layer would result in a decrease in strains (fall below the line), however, these tests were held for 10 days longer than the tests completed by Marcotte and Fleming (2019) and more consolidation (and strain) occurred.

Although the drained tests occurred over a longer period of time (165 days as opposed to 11 days), the resulting SAD and area greater than the 4% strain threshold was significantly less than the undrained tests. The maximum measured strains were also lower for the drained tests. The geomembrane would be expected to strain more under constant stress conditions over a longer time (if unconfined). However, under drained loading there appears to be less differential displacement of the clay/geomembrane interface, thus resulting in lower geomembrane strain. Since all other tests conditions were kept constant, these results of varying the loading rate do support a time-dependent interaction between the clay and geomembrane.

This is not to say that all geomembrane tests are conservative if performed in an undrained manner. The clays tested at the time of writing were limited to low plastic clays with relatively high coefficients of consolidation (higher hydraulic conductivity). Furthermore, differences in geomembrane properties may also play a significant role in the soil-structure interaction, as suggested to by Adesokan et al. (2018). More research is required and currently underway to confirm the relationship between drained and undrained loading for other clay soils.

3.3 Protection Layers and Aggregate

Many others have found a decrease in geomembrane strain with increased protection (Brachman & Sabir 2011; Austin et al. 2014; Tognon et al. 2000). However, there is limited data with protection layers with the SAD method (considering bending strains) as presented in this paper. Undrained tests were also completed with increased protection layers as shown in Figure 8 for the angular gravel above Halton and Battleford Tills.

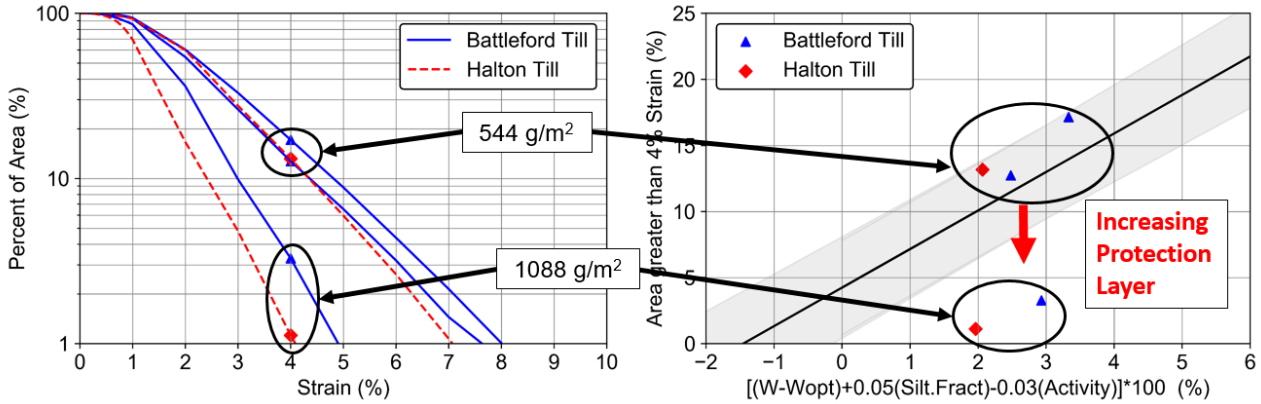

Figure 8: Effect of heavier geotextile protection on geomembrane strain (Test constants: 300 kPa applied load; angular gravel; 1.5 mm geomembrane; undrained loading; held for 11 days at load)

The increase in protection shifts the points below the shaded band as shown in Figure 8. Presumably, there would be another shaded band representing a 1088 g/m^2 protection layer running through the two data points, which would also be dependent on the soil conditions. A change in loading rate may also further reduce the strain, representing another degree of freedom within the plot. With limited data at this time it is unclear what this relationship is and whether it would run parallel to the tests conducted with a 400g/m^2 protection layer as shown in Figure 4.

All tests presented thus far have been completed with the same angular gravel (A. Gravel, Figure 1). It is not uncommon to use either TDA or rounded gravel if available. Figure 9 demonstrates the effect of aggregate as well as protection layer on the development of geomembrane strains. A test pressure of 500 kPa was used for each of the tests, and the soil conditions below remained constant. A 2.0 mm geomembrane was used in the tests with TDA as per recommendations by Marcotte & Fleming (2020) to prevent wire puncture.

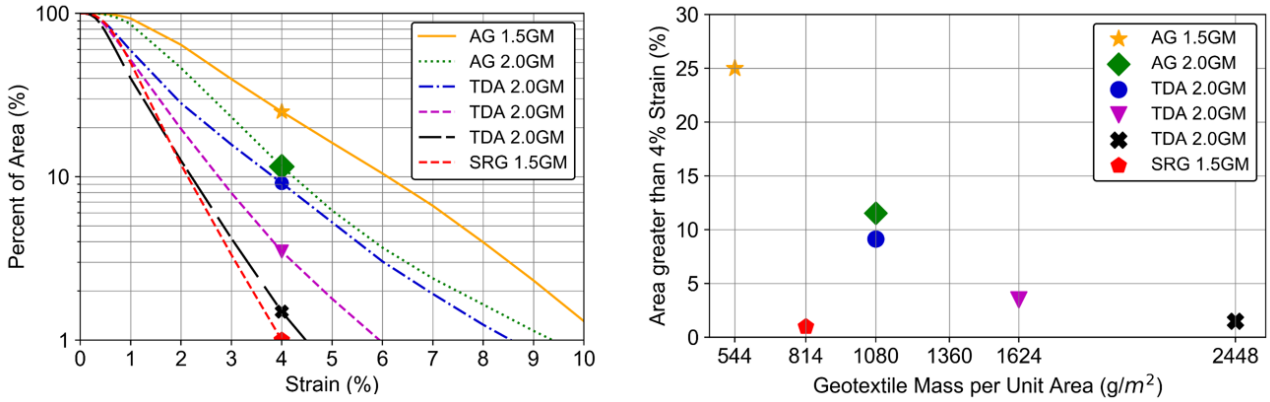

Figure 9: Effect of aggregate on geomembrane strain (Test constants: soil type, water content and shear strength; 500 kPa applied load; undrained loading; held for 24 hours at load) AG – angular gravel; SRG – sub rounded gravel; #GM-geomembrane thickness

The well-graded sub-rounded gravel resulted in the lowest geomembranes strains despite having a relatively light protection layer of 814 g/m^2. Having a more distributed and smaller particle size distribution results in lower contact pressures on the geomembrane (Brachman & Gudina 2008). On the other hand, the increased particle surface area and lower porosity can reduce long-term hydraulic performance when considering leachate clogging (Fleming et al. 1999) and may not be advisable to use as a drainage medium in landfill scenarios. In general, if a gravel aggregate performs well in terms of reducing geomembrane strain, it will likely perform poorly with respect to clogging.

An increase in protection layer resulted lower strains for the tests conducted with TDA, as could be expected. It appears that the TDA performs better than the angular gravel (given the same protection). Marcotte and Fleming (2020) recommended that a minimum 1080 g/m^2 geotextile protection layer with a 2.0 mm geomembrane be used to prevent short-term ductile (large-strain) punctures. Based on the data in Figure 9 at 500 kPa, at the absolute minimum, the same geomembrane/geotextile combination would be required for the use of angular gravel to limit the number of stress cracking holes per hectare and prolong the service life of the geomembrane.

The SAD method works well for comparing relative differences between tests when using a similar size aggregate. The major drawback of this method is the incorrect assumption of only vertical displacements in the underlying equation developed by Tognon et al. (2000). Recent numerical modelling for geomembrane indentations by Eldesouky and Brachman (2018) has indicated that the shape, width (b) and depth (d) of the indentation influences the resulting geomembrane strains when compared to Tognon's method. For deep indentations with large width to depth ratios, Tognon's method overestimates strain. On the other hand, steeper sloped indentations are underestimated using Tognon's method. The over and underestimation of strain was related to the ratio of membrane and bending strains as compared to the numerical approximation, although a distinct relationship or correction factor was not yet developed.

When comparing gravel to TDA, the membrane and bending components of strain can be separated as shown in Figure 10. The membrane strain is always constant for both the top surface and bottom surface of the geomembrane. For the purpose of comparison, the bottom geomembrane bending strain and total bottom strain (sum of membrane and bottom bending strain) are shown in Figure 10.

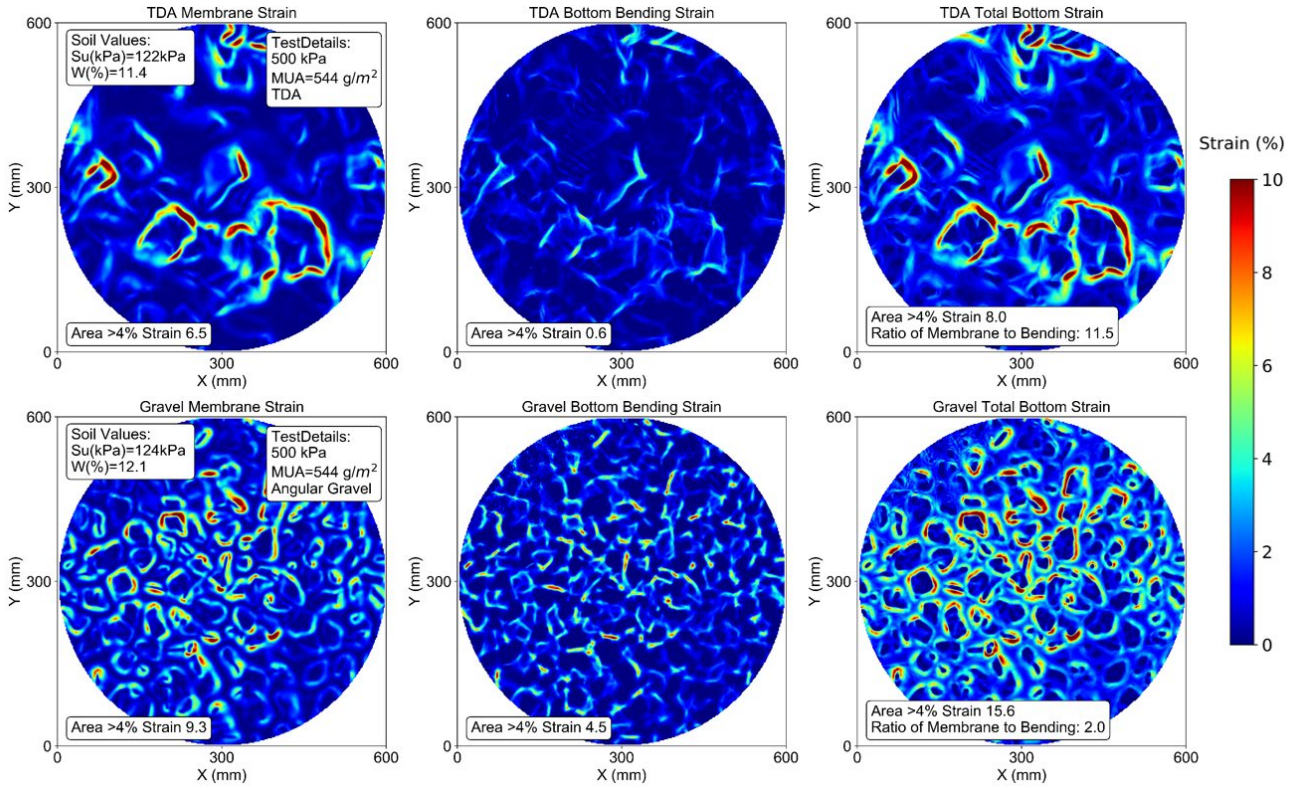

Figure 10: Strain distributions for TDA (top) and gravel (bottom) with separated membrane and bending bottom strains (Test constants: soil type, 1.5 mm geomembrane, water content and shear strength; 500 kPa applied load; undrained loading; held for 24 hours at load)

The TDA particles, being large as compared to gravel, result in wide indentations. Looking to the bending strains, it is evident that the TDA particles do not leave indentations with sharp changes in curvature. By dividing the membrane strain area by the bending strain area exceeding 4% strain, the TDA has significantly more membrane strain contributing to the total Tognon strain – which would be expected for indentations with gradual changes in curvature. By comparing these shaped indentations to similar indentations in the theoretical work by Eldesouky and Brachman (2018), Tognon's method overestimated strain for deep indentations with large width to depth ratios (b/d > 20 and d=10 mm).

On the other hand, the ratio of bending to membrane strains for gravel is closer to one indicating that there is more bending strains relative to membrane strains, indicating steeper indentations. The steeper sloped indentations (b/d=2) when calculated with Tognon's method was determined to underestimate strains (Eldesouky & Brachman 2018).

At the current time, there is no correction factor for Tognon's method, and the Tognon method of calculating strain is still best practice (Eldesouky and Brachman 2018). However, it does appear that the strains in Figure 10 may be overestimated for TDA and underestimated for gravel. In both cases, there is significant amount of the area exceeding not only a 4% threshold, but high strains of greater than 10%, which would likely result in significant stress cracking (Abdelaal et al. 2014). Work is currently ongoing to quantify the over and underestimation of Tognon's method for both TDA and gravel, and ideally provide a correction factor of sorts.

4. CONCLUSIONS

Like many situations in geotechnical and geoenvironmental engineering, an absolute answer for geomembrane strain remains unknown. It must be recognized that the geomembrane is a single component in a complex system - too much attention and resources dedicated to the performance of any one component can have potential negative influences on others. In this paper, the development of geomembrane strains was evaluated using the strain area distribution (SAD) method, but primarily focused on the interactions with the soil subgrade below and protection layers/aggregate above.

The clay below the geomembrane confines and deformations and has a large role in the development of strains. Index clay properties can be related to the magnitude of strains, with higher silt and lower activity leading to higher strains (and vice-versa) when tested under undrained conditions. A 4% increase in compacted water content can triple the area exceeding 4% strain, indicating that weaker and flexible subgrades increase the damage to geomembranes. However, compacting clays with too little water can result in high hydraulic conductivity in compacted clay liners (Benson et al. 1999). It would be advisable to consider both the clay liner and geomembrane when designing specifications for clay liner compaction and perhaps tightening the upper limits of water content or providing an undrained shear strength criteria as well as moisture-density.

Since the clay soils deformations are governed by the principle of effective stress, loading at different rates alter the deformations (stress paths). During geomembrane testing, the loading rate was reduced to represent lifts being placed at a slowly built landfill. Comparing tests performed with slow loading over a 5 month period as opposed to fast testing completed over 11 days (identical test conditions otherwise) the area exceeding a 4% strain threshold was over 2.5 times higher for the tests that lasted 11 days. Maximum strains were also lower for slow loading rate tests. More work is required to confirm the relationship between drained and undrained testing and application to actual landfills. However, it provides an opposite perspective to the premise that short term (undrained) testing is under conservative in all cases.

The aggregate type, size, and shape above the geomembrane were also evaluated. The primary role of large aggregates above liners is removal of hydraulic head while also withstanding biological induced clogging. Small well-graded rounded gravel performs better from the perspective of geomembrane strains. However, use of small aggregate is typically not advised due to regulations and risk of clogging of the collection layer. Large uniform gravel (often crushed and angular) results in the highest geomembrane strains – but also would be preferred to reduce clogging. Tire derived aggregate (TDA) performed better than angular gravel in the development of strains and serves as a valuable resource where high quality crushed stone is both scarce and expensive.

The current methods of calculating strain are known to be based on incorrect assumptions. Based on the ratio of membrane to bending strains as well as the size and shape of the indentations, it is plausible that strains may be overestimated for TDA and underestimated for gravel. Work is currently in progress to test this hypothesis as a correction is not available at this time. A fair comparison between TDA and gravel cannot yet be made until a more accurate method of determining strain is developed.

Finally, the importance of adequate protection must be re-iterated, as has been by others (Rowe et al. 2019; Rowe & Yu; 2019; Brachman et al. 2018). It is not enough to protect the geomembrane against ductile (large strain) punctures but also limit long term tensile strains. At this time, 4% strain is a typical value recommended (Rowe et al. 2019). All of the tests presented herein have some percentage of the area exceeding 4%. Depending on the design life and conditions, it may be unacceptable to have any area exceeding 4%, and very heavy non-woven geotextile protection may be required.

5. REFERENCES

Abdelaal, F. B., Rowe, R. K., & Brachman, R. W. I. (2014). Brittle rupture of an aged HPDE geomembrane at local gravel indentations under simulated field conditions. Geosynthetics International, 21(1), 1–23.

Adesokan, D., Fleming, I., Hammerlindl, A., & McDougall, J. (2019). Strategies for One Dimensional (1D) Compression Testing of Large-Particle-Sized Tire Derived Aggregate. Geotechnical Testing Journal,

Adesokan, D., Marcotte, B., Fleming, I. R., & Tarnowski, C. (2018). A comparison of HDPE geomembranes for response to strains that may be associated with stress cracking. Proceedings 11th International Conference on Geosynthetics
Benson, C. H., & Daniel, D. E. (1990). Influence of Clods on the Hydraulic Conductivity of Compacted Clay. Journal of Geotechnical Engineering, 116(8), 1231–1248.
Benson, C. H., Daniel, D. E., & Boutwell, G. P. (1999). Field Performance of Compacted Clay Liners. Journal of Geotechnical and Geoenvironmental Engineering, 125(5), 390–403.
Brachman, R. W. I., Eastman, M.K., Eldesouky, H. M. G. (2018). Screening Tests to Limit Geomembrane Strain from Gravel Indentations. J. Geotech. Geoenviron. Eng., 144(6)
Brachman, R. W. I., & Sabir, A. (2013). Long-term assessment of a layered geotextile protection layer for geomembranes. J. Geotech. Geoenviron. Eng., 139(5), 752–764.
Brachman, R. W. I., & Sabir, A. (2010). Geomembrane puncture and strains from stones in an underlying clay layer. Geotextiles and Geomembranes, 28(4), 335-343.
Brachman, R. W. I., & Gudina, S. (2008). Gravel contacts and geomembrane strains for a GM/CCL composite liner. Geotextiles and Geomembranes, 26(6), 448–459.
Brummermann, K., Blumerl, W., & Stoewahse, C. (1994). Protection layers for geomembranes: Effectiveness and testing procedures. Proc., 5th International Conference on Geosynthetics, 1003–1006.
Eldesouky, H. M. G., & Brachman, R. W. I. (2018). Calculating local geomembrane strains from a single gravel particle with thin plate theory. Geotextiles and Geomembranes, 46(1), 101-110.
Ewais, A. M. R., Rowe, R. K., Rimal, S., & Sangam, H. P. (2018). 17-year elevated temperature study of HDPE geomembrane longevity in air, water and leachate. Geosynthetics International, 25(5), 525-544.
Fleming, I. R., Rowe, R. K., & Cullimore, D. R. (1999). Field observations of clogging in a landfill leachate collection system. Canadian Geotechnical Journal, 36(4), 685–707.
Hornsey, W. P., and D. M. Wishaw. "Development of a methodology for the evaluation of geomembrane strain and relative performance of cushion geotextiles." Geotextiles and Geomembranes 35 (2012): 87-99.
Hsuan, Y. G., & Koerner, R. M. (1998). Antioxidant depletion lifetime in high density polyethylene geomembranes. Journal of Geotechnical and Geoenvironmental Engineering, 124(6), 532-541.
Marcotte, B. A., & Fleming, I. R. (2020). Damage to geomembrane liners from tire derived aggregate. Geotextiles and Geomembranes, 48(2),198-209.
Marcotte, B. A., & Fleming, I. R. (2019). The role of undrained clay soil subgrade properties in controlling deformations in geomembranes. Geotextiles and Geomembranes, 47(3), 327-335.
Marcotte, B., & Fleming, I. (2018a). Geomembrane puncture and strains from tire derived aggregate for use in landfill applications. Proceedings of the 11th International Conference on Geosynthetics
Marcotte, B., & Fleming, I. (2018b). Geomembrane puncture protection for tire derivedAggregate. Proceedings of GeoEdmonton (71th Canadian Geotechnical Conference)
Marcotte, B., & Fleming, I. (2017). Geomembrane strains and puncture from tire derived aggregate overlying compacted clay. Proceedings of GeoOttawa (70th Canadian Geotechnical Conference)
Narejo, D., Koerner, R. M., & Wilson-Fahmy, R. F. (1996). Puncture protection of geomembranes Part II: Experimental. Geosynthetics International, 3(5), 629-653.
Nosko, V., & Touze-Foltz, N. (2000). Geomembrane liner failure: modelling of its influence on contaminant transfer. Proceedings of 2nd European Geosynthetics Conference: EUROGEO 2000, 2, 557–560.
Peggs, I. D., Schmucker, B., & Carey, P. (2005). Assessment of Maximum Allowable Strains in Polyethylene and Polypropylene Geomembranes. Waste Containment and Remediation.
Rowe, R. K., Brachman, R. W. I., Irfan, H., Smith, M. E., & Thiel, R. (2013). Effect of underliner on geomembrane strains in heap leach applications. Geotextiles and Geomembranes, 40, 37–47.
Rowe, R.K., Priyanto, D., Poonan, R., 2019. Factors affecting the design life of HDPE geomembranes in an LLW disposal facility. In: WM2019 Conference, Phoenix, Arizona, USA, 15p.
Rowe, R. K. (2012). Short-and long-term leakage through composite liners. The 7th Arthur Casagrande Lecture. Canadian Geotechnical Journal, 49(2), 141-169.
Rowe, R. K. (2005). Long-term performance of contaminant barrier systems. Géotechnique, 55(9), 631–678.
Rowe, R. K., & Yu, Y. (2019). Magnitude and significance of tensile strains in geomembrane landfill liners. Geotextiles and Geomembranes, 47(3), 439-458.
Seeger, S., & Müller, W. (1996). Requirements and testing of protective layer systems for geomembranes. Geotextiles and Geomembranes, 14(7-8), 365-376.
Tognon, A. R., Kerry Rowe, R., & Moore, I. D. (2000). Geomembrane Strain Observed in Large-Scale Testing of Protection Layers. Journal of Geotechnical and Geoenvironmental Engineering, 126(12), 1194–1208.
Yesnik, C., Marcotte, B., Fleming, I. (2019). A low-cost automated SWCC device and data analysis procedure for unsaturated soils exhibiting volume change. Proceedings of Geo St. Johns